

# Initial Magnetic Field Distribution Around High Rectangular Bus Bars

Grigore A. Cividjian<sup>1</sup>

**Abstract:** The one-dimensional transient electromagnetic field in and around a system of two nonmagnetic homogenous rectangular high thin bars can be analytically evaluated if the ratio of average initial magnetic field on the two sides of thin bar, or of the ratio of initial magnetic fields in middle of the bar height is known. In this paper, using appropriate conformal mappings, an exact analytical solution for these ratios are proposed in the case of very thin bars. Obtained values are compared with FEM results for relatively thick bars.

**Keywords:** Conform mapping, Initial magnetic field, Elliptic integrals.

## 1 Introduction

The problem of transient electromagnetic fields for a system of two infinite-high and long non-magnetic bars in cases of current and voltage step application is completely studied and brilliantly solved in [1], considering the magnetic field on internal side of the bars constant and evenly distributed and on the external side of the bars equal to zero.

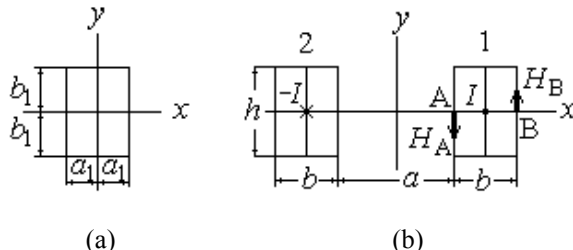


**Fig. 1 – Single bar and the set of two bars.**

In [6], considering the magnetic field in the central part of one-dimensional bar, all these results are extended for the case of finite height of the bars. The obtained in [6] results depend on the (considered almost constant) ratio  $\eta(t)$  of the tangential magnetic fields on bar sides. The final ( $t \rightarrow \infty$ ) values of this ratio are exactly determined in [6], using expression (1) of the vertical component of

<sup>1</sup>University of Craiova, 107, Bd. Decebal, 200440 Craiova, Romania; E-mail: gcividjian@elth.ucv.ro

the magnetic field produced by a uniformly distributed direct current in single bar. The vertical component of the steady state magnetic field of single bar with the cross-section  $2 a_1 \times 2 b_1$  carrying a direct current  $I$  with constant density  $j$  is given in [2]:

$$H_y(x, y) = \frac{j}{2\pi} \begin{bmatrix} (x + a_1) \left( \arctan \frac{y + b_1}{x + a_1} - \arctan \frac{y - b_1}{x + a_1} \right) \\ -(x - a_1) \left( \arctan \frac{y + b_1}{x - a_1} - \arctan \frac{y - b_1}{x - a_1} \right) \\ + \frac{y + b_1}{2} \ln \frac{(x + a_1)^2 + (y + b_1)^2}{(x - a_1)^2 + (y + b_1)^2} - \frac{y - b_1}{2} \ln \frac{(x + a_1)^2 + (y - b_1)^2}{(x - a_1)^2 + (y - b_1)^2} \end{bmatrix}, \quad (1)$$

$$j = \frac{I}{4a_1 b_1}.$$

Using the supplementary function:

$$\phi(x, y) = (x + y) \arctan \frac{1}{2(x + y)} - x \arctan \frac{1}{2x} + \frac{1}{4} \ln \left[ \frac{1 + 4(x + y)^2}{1 + 4x^2} \right], \quad (2)$$

$$\frac{\partial \phi(x, y)}{\partial y} = \arctan \frac{1}{2(x + y)},$$

the final values of ratio  $\eta_\infty = \left| \frac{H_B}{H_A} \right|_{t=\infty}$  can be exact calculated with the following equation (Fig. 1b):

$$\eta_\infty(a, b, h) = \frac{\phi\left(0, \frac{b}{h}\right) - \phi\left(\frac{a+b}{h}, \frac{b}{h}\right)}{\phi\left(0, \frac{b}{h}\right) + \phi\left(\frac{a}{h}, \frac{b}{h}\right)}. \quad (3)$$

For thin bars, using the l'Hôpital's rule, the following equation is obtained for the final ratio of magnetic fields in the middle of the two sides of very thin bars:

$$\eta_\infty|_{b=0} = \frac{\frac{\pi}{2} - \arctan \frac{h}{2a}}{\frac{\pi}{2} + \arctan \frac{h}{2a}}. \quad (4)$$

In [6] the same formula was obtained as the limit case for  $b \rightarrow 0$  in the equation

$$\eta_{0m} = \left| \frac{H_B}{H_A} \right|_{t=0} \approx \frac{\arctan \frac{h}{b} - \arctan \frac{h}{2a+b}}{\arctan \frac{h}{b} + \arctan \frac{h}{2a+b}} \quad (5)$$

obtained from the condition of zero magnetic field in the centre of the bar and considering the initial current as two evenly distributed sheets of current on the surface of each bar and proposed for roughly evaluation of initial ratio of magnetic fields in middle of the bar.

A slightly more exact formula can be obtained, considering the condition of zero magnetic field not in the centre of the bar, but closer to the external side, where the magnetic field remains zero up to the end of field penetration process:

$$\eta_2(\eta) = \frac{\arctan \left( \frac{1+\eta}{2} \frac{h}{b} \right) - \arctan \left[ h / \left( 2a + \frac{2b}{1+\eta} \right) \right]}{\arctan \left( \frac{1+\eta}{2\eta} \frac{h}{b} \right) + \arctan \left[ h / \left( 2(a+b) + \frac{2b}{1+\eta} \right) \right]}, \quad (6)$$

$$\eta = \eta_\infty.$$

In the case of current step injection, considering a better approximation than in [6] for the magnetic field in the point A, we can write for transient fields in the middle part of high bar with electrical conductivity  $\sigma$  and magnetic permeability  $\mu$  the following equations, as functions of space and time relative units:

$$H_A \approx \frac{I}{(1+\eta)(h+b)}, \quad H_B = \eta H_A,$$

$$E_0 = \frac{I}{\sigma b h} \approx \frac{1+\eta}{\sigma} \left( \frac{1}{b} + \frac{1}{h} \right) H_A, \quad b \ll h,$$

$$\xi = \frac{x}{b}, \quad \tau = \mu \sigma b^2, \quad \theta = \frac{t}{\tau},$$

$$H_y(\xi, \theta) = H_A \left[ \frac{2}{\pi} \sum_{k=1}^{\infty} (-1)^k \frac{\eta \sin(k\pi\xi) - \sin(k\pi(1-\xi))}{k} e^{-(k\pi)^2 \theta} \right], \quad (7)$$

$$E_z(\xi, \theta) = \frac{E_0}{1+\eta} \left[ \frac{1+\eta}{2} + \sum_{k=1}^{\infty} (-1)^k [\eta \cos(k\pi\xi) + \cos(k\pi(1-\xi))] e^{-(k\pi)^2 \theta} \right].$$

Since  $\eta$  is time varying quantity, for initial period of the process  $\eta_0$  must be considered. For better determination of  $\eta_{0m}$  and  $\eta_{0av}$  a static problem was solved using FEM. A sample of the magnetic field initial distribution around the bar is given in Fig. 5. But even with many nodes, the magnetic field in the corners of the bars is badly determined. This is why in the next section an exact analytical solution is presented, unfortunately valid only for the case of very thin bars.

## 2 External Magnetic Field Around Thin Bar

In the case of current step excitation, the initial magnetic field is only external and the last flux line coincides with conductor contour. In quasi-stationary approximation its magnetic vector potential  $A$  satisfy the Laplace equation. The distribution of the magnetic field values along the conductor contour will be analyzed in first quadrant of Fig. 1b, by using a conformal mapping of non-conducting domain in a rectangle. The boundary conditions of the field problem are given in Fig. 5.

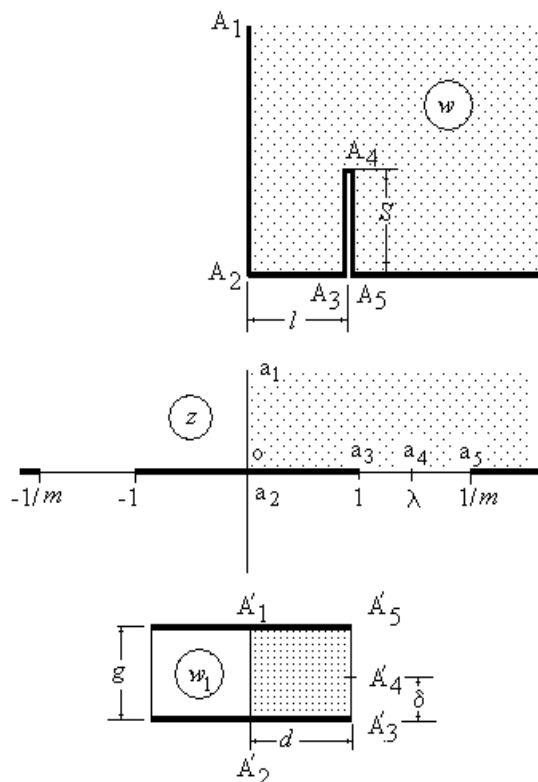


Fig. 2 – Conformal transforms domains.

In the case of infinitely thin bars ( $b \rightarrow 0$ ), the domain of interest can be transformed in the upper half plane using the analytical function (Fig. 2) [4, 5]:

$$w(z) = \frac{2l}{\pi} \left[ K'E(z, m) - (K' - E')F(z, m) \right]. \quad (8)$$

Here  $K'$ ,  $E'$  are complete elliptic integrals and  $F$ ,  $E$  are incomplete elliptic integrals of first and second kind and modulus  $m$ .

The abscissa  $\lambda$  of the point  $a_4$ , corresponding to the top of the bar is:

$$\lambda = \frac{1}{m} \sqrt{\frac{E'}{K'}} \quad \lambda \in \left[ 1, \frac{1}{m} \right]. \quad (9)$$

Replacing (9) in (8) the following equation is obtained:

$$\begin{aligned} 1 + \frac{S}{l} i &= \frac{2}{\pi} \left[ K'E(\lambda, m) - (K' - E')F(\lambda, m) \right] = \\ &= \frac{2}{\pi} K' \left[ E(\lambda, m) - (1 - m^2 \lambda^2) F(\lambda, m) \right]. \end{aligned} \quad (10)$$

For  $\cosh(\chi) \in (1, 1/m]$  the following equation will be considered [3, 7]:

$$F\left(\frac{\pi}{2} + i\chi, m\right) = K(m) + iF\left(\arcsin \frac{\tanh \chi}{m'}, m'\right). \quad (11)$$

where  $m'$  is the co-modulus of the elliptic integral. Or,

$$F(x, m) = K(m) + iF\left(\frac{\sqrt{x^2 - 1}}{xm'}, m'\right). \quad (12)$$

In particular,

$$F\left(\frac{1}{m}, m\right) = K(m) + iK'(m'). \quad (13)$$

There is also the Legendre identity:

$$K'(E - K) - KE' = \frac{\pi}{2}. \quad (14)$$

Using the substitution

$$x = \frac{\sqrt{1 - m'^2 t^2}}{m}, \quad (15)$$

the following equations result for  $x \in (1, 1/m)$

$$F(x, m) = K(m) + i \left[ K'(m) - F\left(\frac{\sqrt{1 - m^2 x^2}}{m'}, m'\right) \right], \quad (16)$$

$$E(x, m) = E(m) + i \left[ K'(m) - E'(m) - F\left(\frac{\sqrt{1-m^2x^2}}{m'}, m'\right) + E\left(\frac{\sqrt{1-m^2x^2}}{m'}, m'\right) \right]. \quad (1)$$

Replacing these expressions in (10) we can obtain the geometrical ratio  $S/l$  as function of the co-modulus  $m'$ :

$$\frac{S}{l} = \frac{2}{\pi} \left[ K(m') E\left(\frac{\sqrt{1-\frac{E(m')}{K(m')}}}{m'}, m'\right) - E(m') F\left(\frac{\sqrt{1-\frac{E(m')}{K(m')}}}{m'}, m'\right) \right]. \quad (18)$$

For  $m < 0.3$ , we can use the approximations [3]:

$$\begin{aligned} K'(m) &\approx \left(1 + \frac{m^2}{4}\right) \cdot \Lambda, \\ E'(m) &\approx 1 + \frac{m^2}{4}(2\Lambda - 1), \quad \Lambda = \ln \frac{4}{m}, \\ E\left(\frac{\sqrt{1-\frac{E(m')}{K(m')}}}{m'}, m'\right) &\approx \sqrt{1 - \frac{1}{\Lambda}} \approx 1 - \frac{1}{2\Lambda}, \\ F\left(\frac{\sqrt{1-\frac{E(m')}{K(m')}}}{m'}, m'\right) &\approx \operatorname{arth} \sqrt{1 - \frac{1}{\Lambda}} \approx \frac{1}{2} \ln(4\Lambda) - \frac{1}{8\Lambda}. \end{aligned} \quad (19)$$

With these approximations, (18) can be simplified as follows:

$$\frac{S}{l} \approx \frac{2}{\pi} \left[ \Lambda - \frac{1 + \ln(4\Lambda)}{2} + \frac{1}{8\Lambda} \right], \quad m = 4e^{-\Lambda} < 0.3. \quad (20)$$

For  $S/l > 2$  ( $m < 0.03$ ) with 1% approximation, the following formula can be used for modulus evaluation:

$$\begin{aligned} \frac{S}{l} &\approx -0.6 \ln(m) - 0.25, \\ m &\approx \exp\left(-\frac{S/l + 0.25}{0.6}\right), \quad m < 0.03. \end{aligned} \quad (21)$$

The configuration from the plane  $z$  can also be transformed in a  $d \times g$  rectangle with the function [7]:

$$w_1(z) = \frac{d}{K(m)} F(z, m). \quad (22)$$

The images in  $w_1$ -plane of the points  $a_4$  and  $a_5$  from  $z$ -plane will be:

$$\begin{aligned} d + i\delta &= \frac{d}{K(m)} F(\lambda, m), \\ d + ig &= \frac{d}{K(m)} F\left(\frac{1}{m}, m\right) = d\left(1 + i\frac{K'}{K}\right). \end{aligned} \quad (23)$$

In the rectangle obtained in the  $w_1$ -plane the field is uniform and the  $A'_3 A'_5$  side is a field line. The ratio of magneto-motive force (mmf) on the left side of bar to the total mmf, on both sides, will be:

$$\frac{\delta}{g} = \frac{F(\lambda, m) - K(m)}{F(1/m, m) - K(m)} = \frac{F(\lambda, m) - K(m)}{iK'(m)}. \quad (24)$$

The ratio of the average tangential magnetic field on right side ( $H_{Bav}$ ) to the average tangential magnetic field on the left side ( $H_{Av}$ ) of the bar at  $t = 0$  will be the same as the ratio of corresponding magneto motive forces (since both sides has the same height  $h$ ). In the  $w_1$ -plane the magnetic field along the side  $A'_3 A'_5$  is uniform and the ratio of magneto-motive forces along the two sides of the infinite thin bar will be the same as the ratio of corresponding segments ( $A'_4 A'_5$  and  $A'_3 A'_4$ ) length:

$$\eta_{0av}(m) = \left| \frac{H_{Bav}}{H_{Av}} \right|_{t=0+} = \frac{g - \delta}{\delta} = \frac{iK'(m)}{F(\lambda, m) - K(m)} - 1. \quad (25)$$

The ratios  $h/a$  (18) and  $\eta_{0av}$  (21) are plotted in Fig. 3 as function of modulus  $m$ .

The magnetic field intensity in  $w$ -plane is:

$$H_w = H_{w1} \frac{dw_1}{dw} = H_{w1} \frac{dw_1}{dz} \cdot \frac{dz}{dw}. \quad (26)$$

Taking into account the definitions of  $w$ ,  $w_1$  and  $\lambda$ , the derivatives are:

$$\frac{dw_1}{dz} = \frac{d}{K(m)} \frac{1}{\sqrt{(z^2 - 1)(1 - m^2 z^2)}}, \quad (27)$$

$$\begin{aligned} \frac{dw}{dz} &= \frac{2l}{\pi} K'(m) \left[ \sqrt{\frac{1 - m^2 z^2}{z^2 - 1}} - \frac{1 - m^2 \lambda(m)^2}{\sqrt{(z^2 - 1)(1 - m^2 z^2)}} \right] = \\ &= \frac{2l}{\pi} \frac{m^2 K'(m) [\lambda(m)^2 - z^2]}{\sqrt{(z^2 - 1)(1 - m^2 z^2)}}. \end{aligned} \quad (28)$$

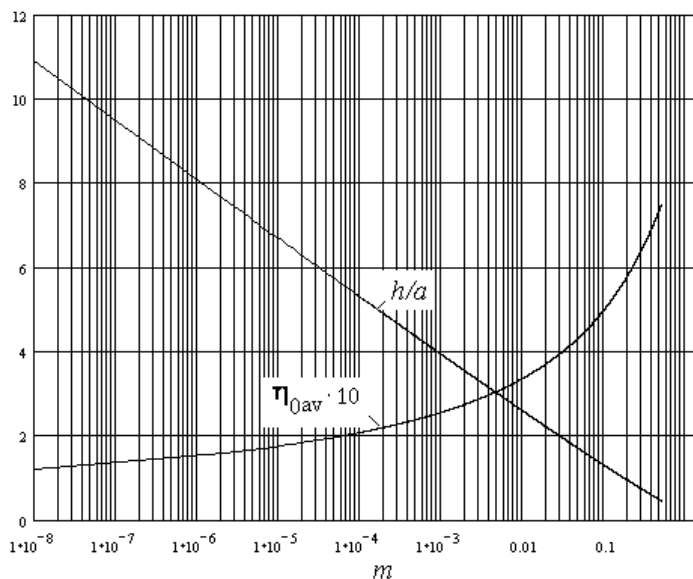


**Fig. 3 – Ratio of average initial magnetic fields (25) and  $h/a$  versus modulus  $m$  (18).**

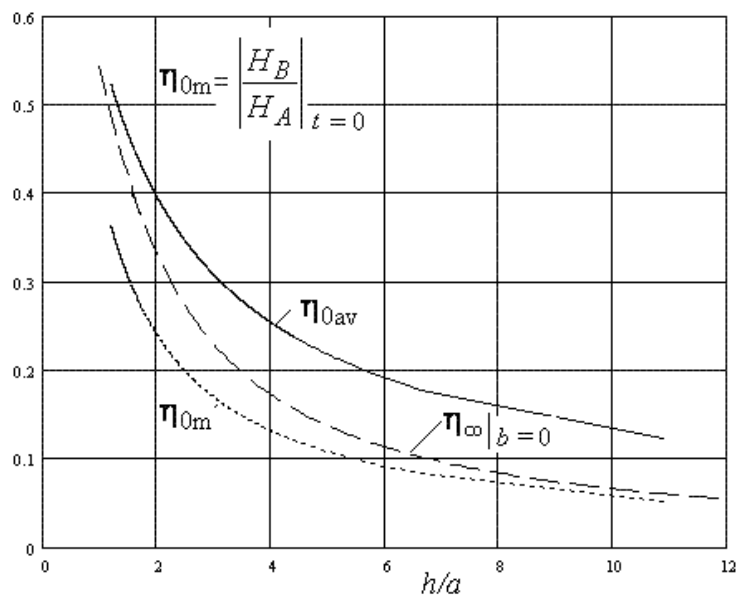


**Fig. 4 – Ratios of initial magnetic fields versus  $h/a$ .**

Consequently, the magnetic field along both sides of the bar, with current  $I$  (in the  $w$ -plane), as a function of the  $z$ -plane coordinates, has the following expression:

$$\begin{aligned} H(x) &= \frac{\pi}{2} \frac{d}{l} \frac{H_0}{K' K m^2 (\lambda^2 - x^2)} = \frac{\pi}{4l} \frac{I}{K'^2 m^2 (\lambda^2 - x^2)}, \\ H(x) &= \pi \frac{S}{l} \frac{H_{av}}{K'(m)(E' - K' m^2 x^2)}, \quad H_{av} = \frac{I}{4S} \approx \frac{I}{2(h+b)}. \end{aligned} \quad (29)$$

The modulus  $m$  depends on the ratio  $S/l$  (18), (20), (21) and  $H_{av}$  is the average initial magnetic field around the bar.

The ratio of the initial magnetic fields on the two sides in the middle of bar height will be:

$$\eta_{0m}(m) = \left| \frac{H_B}{H_A} \right|_{t=0} = \frac{\lambda^2(m) - 1}{1 - m^2 \lambda^2(m)} m^2. \quad (30)$$

In Fig. 4 the values of the ratios  $\eta_{0av}$ ,  $\eta_{0m}$  calculated with (25) and (30) are given as function of  $h/a$ . The dashed line is the final value ( $t \rightarrow \infty$ ) of this ratio  $\eta_\infty$  for very thin bar ( $b = 0$ ), calculated with (4). From this figure it can be observed that in general the ratio of lateral magnetic fields increases from their initial value  $\eta_0$  to the final value  $\eta_\infty$  and for large values of  $h/a$  this variation is negligible. For small  $h/a$ , the values given by simple formula (4) are closer to  $\eta_{0av}$  and for large  $h/a$  they are closer to  $\eta_{0m}$ .

Calculations made with numerical methods [8, 9] show that for thick bars ( $b > 0$ ), the initial values of  $\eta_{0m}$  are smaller than for  $b = 0$  if they are considered in Fig. 4 as functions of  $h/a$  but they are larger than the values for  $b = 0$  and closer to them if instead of the  $h/a$  the ratio  $(h+b)/a$  is considered. So, the value of  $\eta_{0m}$  for thick bars is between the values of  $\eta_{0m}$  given in Fig. 4 for  $h/a$  and  $(h+b)/a$ :

$$\begin{aligned} \eta_{0m} \left( \frac{h+b}{a} \right) &< \eta_{0m}|_{b>0} < \eta_{0m} \frac{h}{a}, \\ \eta_{0m}|_{b>0} &\approx \eta_{0m} \left( \frac{h+b}{a} \right), \quad b < h. \end{aligned} \quad (31)$$

The values of  $\eta_{0av}$  for thick bars are always smaller than the values given in Fig. 4 for  $(h+b)/a$ .

For thick bars with  $0 < b < h$  the following simple equation is proposed in [8]:

$$\eta_{0m}(x) \approx (0.7 + 0.02x) \frac{\frac{\pi}{2} - \arctan\left(\frac{x}{2}\right)}{\frac{\pi}{2} + \arctan\left(\frac{x}{2}\right)}, \quad x = \frac{h+b}{a}, \quad b < h. \quad (32)$$

### 3 Example: Numerical Solution for Thick Bar

To illustrate the influence of the bar thickness on magnetic fields ratios, in Fig. 5 is shown a numerical solution (obtained using FEMM with asymptotic boundary conditions on circular outer boundary) for a relatively thick bar:  $b/a = 0.5$  and  $h/a = 5$ . A uniform mesh size  $b/10$  was used and the radius of outer boundary is  $r_0 = 5h$ . No supplementary mesh refinement near the border or corner was used, except the automatically made by FEMM.

The ratio of the initial magnetic fields in the middle of the bar height ( $\eta_{0m}$ ) results 0.095, close enough to the analytical value ( $\sim 0.1$ ) given in Fig. 4 for  $(h+b)/a = 5.5$ . But for  $\eta_{0av}$  the errors are much larger. Even if instead of  $h/a$  the value  $(h+b)/a$  is considered, the ratio of the average magnetic fields, obtained by finite element method, is much smaller than the theoretical value: 0.15 versus 0.20. This happens probably because in the corner of the bar the magnetic field theoretically tends to infinity and the numerical errors are very large, even when using many nodes.

This example shows once more the utility of exact theoretical solution.

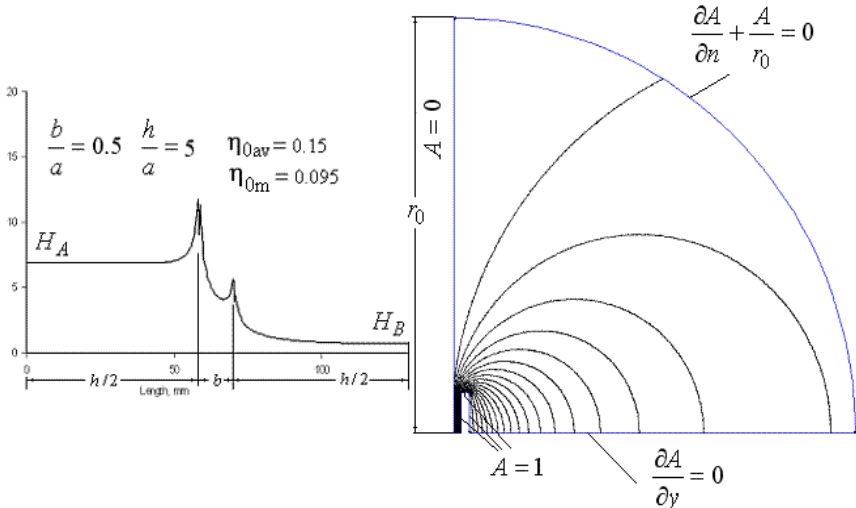


**Fig. 5 – Pattern of the magnetic field (numerical solution).**

## 4 Conclusion

1. For this open boundary problem the values of the initial magnetic field cannot be exactly determined with FEM near the corners, even if a large number of nodes is used. Therefore, an exact analytical solution, (even if only for a very thin bar, with  $b < h/20$ ) is welcomed.
2. The exact values of  $\eta_{0m}$  and  $\eta_{0av}$  for  $b = 0$  are given in Fig. 4 in function of  $h/a$ . Using  $h+b$  instead of  $h$  they can be used for ratios evaluation for relatively small  $b$ .
3. The initial magnetic field ratio depends mainly on the geometrical ratio  $h/a$  and there is a large discrepancy between ratios of the fields in the middle of the bar  $\eta_{0m}$  and the ratios of average magnetic field on both sides of the bar  $\eta_{0av}$ .
4. The former approximate formula (4), obtained for  $\eta_0$ , gives values between the ratio of the initial fields in the middle of the bar and the ratio of the average fields on lateral sides of the bar, closer to  $\eta_{0av}$  for  $h/a < 2$  and closer to  $\eta_{0m}$  for  $h/a > 3$ . All these ratios given by (4), (25) and (30) are plotted in Fig. 4.
5. In Fig. 4 can be seen the total variation in time (from  $t = 0$  to  $t = \infty$ ) of the ratio  $\eta$ , from  $\eta_{0m}$  to  $\eta_\infty$  for the middle part of thin bar. It can be observed that at least in the case of thin high bars the ratio  $\eta$  increases from the initial value  $\eta_{0m}$  to the final value  $\eta_\infty$  with about 50% for  $h = a$  and rest almost constant for  $h > 10a$ . This means that the assumption considering the magnetic field constant during the field penetration on each surface in the middle part of high bar, adopted in [1] and [6] is justified.

## 4 References

- [1] A. Tugulea: Transient Electromagnetic Field in Massive Bus Bars - Transient Parameters, St. Cerc. Energ. Electr., Vol. 22, No. 1, Bucharest, 1972, pp. 67 – 93. (In Rumanian).
- [2] K.J. Binns, P.J. Lawrenson: Analysis and Computation of Electric and Magnetic Field Problems, Pergamon Press, Oxford, UK, 1973.
- [3] E. Janke, F. Emde, F. Losh: Tables of Higher Functions, Teubner, Stuttgart, Germany, 1960.
- [4] W. Koppenfels, F. Stallmann: Praxis der Konformen Abbildung, Springer-Verlag, Berlin, Germany, 1959. (In German).
- [5] V.I. Lavrik, V.I Savenkov: Handbook on Conformal Mappings, Naukova, Kiev, Ukraine, 1970. (In Russian).
- [6] G.A. Cividjian: Current Distribution in Rectangular Busbars, Revue Roumaine des Sciences Techniques, Série Electrotechnique et Energetique, Vol. 48, No. 2-3, 2003, pp. 313 – 320.
- [7] G.A. Cividjian, A.G. Cividjian: Constriction and Corner Permeances for Finite Domains, IEEE Transaction on Magnetics, Vol. 42, No. 12, Dec. 2006, pp. 3825 – 3831.

- [8] G.A. Cividjian: Initial Magnetic Field Distribution Around Rectangular Busbars, Annals of the University of Craiova, Electrical Engineering Series, No. 32, 2008, pp. 68 – 71.
- [9] A.I. Dolan, G.A. Cividjian: Numerical Determination of Rectangular Busbars Transient Parameters, Annals of the University of Craiova, Electrical Engineering Series, No. 32, 2008, pp. 210 – 215.